Separation Science and Technology
Publication details, including instructions for authors and subscription information:
http://www.informaworld.com/smpp/title~content=t713708471

Palmitoleic Acid Enrichment of Seabuckthorn (Hippophaë rhamnoides L.) Pulp Oil by Crystallization Process

Luis-Felipe Gutiérrez[a]; Khaled Belkacemi[a]
[a] Soils and Agri-Food Engineering Department, Nutraceuticals and Functional Foods Institute (INAF), Université Laval, Sainte-Foy, Québec, Canada

To cite this Article Gutiérrez, Luis-Felipe and Belkacemi, Khaled(2008) 'Palmitoleic Acid Enrichment of Seabuckthorn (Hippophaë rhamnoides L.) Pulp Oil by Crystallization Process', Separation Science and Technology, 43: 8, 2003 — 2022
To link to this Article: DOI: 10.1080/01496390802064091
URL: http://dx.doi.org/10.1080/01496390802064091

Separation Science and Technology, 43: 2003–2022, 2008

ISSN: 0149-6395 print/1520-5754 online
DOI: 10.1080/01496390802064091

Taylor & Francis
Taylor & Francis Group

Palmitoleic Acid Enrichment of Seabuckthorn (Hippophaë rhamnoides L.) Pulp Oil by Crystallization Process

Luis-Felipe Gutiérrez and Khaled Belkacemi
Soils and Agri-Food Engineering Department, Nutraceuticals and Functional Foods Institute (INAF), Université Laval, Sainte-Foy, Québec, Canada

Abstract: Seabuckthorn pulp oil was fractionated using a crystallization process with acetone under controlled cooling rate of 0.25°C/min without agitation at different crystallization temperatures ranging from −15 to 15°C. The obtained liquid (LF) and solid (SF) fractions were analyzed for their fatty acid and triacylglycerol compositions and their melting profiles were characterized. Fractionation at −15°C yielded about 20% of LF where palmitoleic acid represented 53% of total lipids. The SF fraction was mainly rich in palmitic acid. LF were richer in triacylglycerol with acyl carbon numbers of 50 and 52 (C50 and C52) than SF, which contained a higher amount of C48. The melting curves of LF and SF showed multiple endothermic transitions.

Keywords: Crystallization; Fatty acids; *Hippophaë rhamnoides*; Melting curves; Palmitoleic acid; Seabuckthorn; Solvent fractionation; Triacylglycerols

INTRODUCTION

The recent interest in pharmaceutical applications of unsaturated fatty acids pushed the research towards the exploitation of new sources of fatty substrates. Since monounsaturated fatty acids such as palmitoleic (Cl6:1), undecylenic (C11:1), and tridecenic (C13:1) acids showed the potential to

Received 4 November 2007; accepted 12 February 2008.
Address correspondence to Khaled Belkacemi, Soils and Agri-Food Engineering Department, Nutraceuticals and Functional Foods Institute (INAF), Université Laval, Sainte-Foy, Québec, G1K 7P4, Canada. Tel.: 418-656-2131: Fax: 418-656-3327; E-mail: khaled.belkacemi@sga.ulaval.ca

prevent diseases connected to the cerebral and cardiovascular functions, and to improve the function of the vascular soft cells (1), it is expected that they will find applications in the human nutrition and medicine.

Among these acids, palmitoleic acid is an omega-7 monounsaturated fatty acid present in animal as well as vegetal kingdoms. It is present in interesting quantities in marine animals such as sharks and seals whereas its content is negligible in traditional vegetable oils (1% in soya, cotton seed oils and olive oils). The most available source of this acid is the oil of macadamia nuts (*M. integrifolia* and *M. tetraphylla*) which contain 17 to 34% (2). Interestingly, the most important source of palmitoleic acid is the Sea buckthorn oil pulp (SBPO) (3).

The current application of palmitoleic acid is in cosmetics. It is reported that the human epidermic lipids contain up to 20% w/w, which would explain its use for fine cosmetics in skin care (4). This acid was regarded as the most prevalent acid exhibiting high antimicrobial activity. It can be used in topical formulas for the treatment of secondary gram-positive bacterial infections and as gram-positive antimicrobial preservative for skin and hair treatments (5). Moreover, palmitoleic acid does not present any toxicity and was reported to control the cell viability by interacting within various reaction mechanisms leading to the apoptosis (6). Even if the association of fatty acids with the prostate cancer was more or less consistent (7,8), reduction in the risk of this cancer with palmitoleic acid uptake in the food diet was successfully demonstrated (9).

The extraction of this fatty acid is technically demanding (10). A process intensification allowing the increase of palmitoleic acid levels and the diminution of palmitic acid concentrations is highly desirable and could make the SBPO utilization more advantageous. Rüsch gen. Klaas and Meurer (11) reported a palmoleic acid increase of about 50%, using a procedure comprising oil extraction from sea buckthorn pomace, followed by oil transesterification, fractional distillation, and urea crystallization. In spite of the high concentration of palmitoleic acid obtained in the final ester concentrate (81.9%), the low yield of the process (about 4%) and the possible formation of carcinogenic ethyl or methyl carbamates when using urea (12) could limit its application in the food and pharmaceutical industries. Furthermore, this process destroys the chemical nature of triacylglycerols and the final product is not claimed as oil.

Our recent work on the oil extraction of Sea buckthorn fruits demonstrated that the pulp oil contains 41% of palmitoleic acid and 31% of palmitic acid. These two acids constitute up to 75% of the pulp oil. The latter can be extracted with relatively high yields of 35% w/w dry basis (13,3). SBPO exhibits a wide melting range, from approximately $-30^{\circ}C$ to $20^{\circ}C$ (13). This may allow the fractionation by crystallization

of a series of triacylglycerols at temperatures below their melting points by rigorous control of the oil cooling rate (14).

Mainly two types of fractionation processes exist: dry and solvent fractionation (15). Although dry fractionation is the simplest and most economical technology, separation of the fat crystals from the liquid matrix is often difficult and incomplete (16). Preliminary dry fractionation experiments of SBPO showed that the phase separation is very difficult owing to the high viscosity of the SBPO at temperatures below 0°C and the formation of crystal matrixes occluding some impurities of low-melting triacylglycerols. Solvent fractionation, using mainly acetone or hexane, is commercially applied to produce specialty oils and some salad oils from a wide selection of edible oils (17,18). According to Timms (15), the main advantages of using a solvent are the short crystallization time and the high separation efficiency. As expected, the fractionation by crystallization of SBPO and its enrichment in palmitoleic acid were hardly addressed.

The main objective of this work is to investigate the enrichment of SBPO in palmitoleic acid by means of solvent crystallization process using acetone. More specifically, it tackles on the crystallization temperature effect on the yield, fatty acid and TAG compositions as well as melting profiles of the obtained fractions.

MATERIALS AND METHODS

Berries

Seabuckthorn berries (Hippophaë rhamnoides L. cv. Indian-Summer) from Sainte-Anne-de-Beaupré (Québec, Canada) were hand cleaned and stored at −30°C in sealed plastic bags until the beginning of the experiments.

Air-Drying of Seabuckthorn Berries

Frozen ground berries were placed in a perforated drying tray. Starting with 900 g berries, air-drying experiments were conducted at 50°C and 1.0 m/s air velocity for 24 h, using a laboratory tray drier (Model UOP8-G, Armfield, Hampshire England). The dried product was crushed in a mortar to facilitate the separation of seeds from the pulp. Special caution was exercised in order to avoid seeds damage. A 10 mesh (2 mm) sieve (Canadian Standard Sieve Series, W.S. Tyler, St Catharines, ON, Canada) was used to separate most seeds from dried pulp. Pulp residues adhered to seeds, were hand-separated and crushed in a mortar.

The air-dried pulp was stored at $-20^{\circ}C$ in plastic containers until oil extraction.

SBPO Extraction

The pulp of air-dried seabuckthorn was extracted with hexane at 50°C in sealed flasks under continuous agitation for 24 h. After extraction, the flask contents were filtered. The solid residue was discarded while the filtrate containing the majority of the solvent and the extracted oil was recovered as a micella. The solvent in the micella was removed using a rotary film evaporator (Büchi R-205, Cole-Parmer, Vernon Hills, IL, USA). The oil (SBPO) was collected, evaporated under nitrogen, and stored in sealed amber glass vials at $-20^{\circ}C$ until crystallization processes and analysis. The detailed procedure of the extraction process was reported elsewhere in our previous works (12,13).

Solvent Crystallization Process

Samples of SBPO ($\sim$1.5 g) were placed into a 15-mL polypropylene centrifuge tube and mixed with acetone, using a 1/5 m/v oil to solvent ratio. Crystallization processes were carried out at different temperatures (15, 5, -1, -5, -10, and $-15^{\circ}C$) without agitation. The centrifuge tubes were placed into a thermoregulated bath (HAAKE-C, HAAKE, Germany) containing ethylene-glycol/water mixture. The bath cooling rate was controlled by means of a digital temperature programmer (HAAKE PG 41, HAAKE, Germany) as follows: from 30°C (isothermal for 30 min) to the crystallization temperature (T_C) at 0.25°C/min, and held at this temperature for about 24 h. The bath temperature was registered over time using a temperature data logger (HOBO H8 4-Channel Outdoor/Industrial External Input Logger, Onset Computer Corporation, USA). At the end of the crystallization process, liquid (LF) and solid (SF) fractions were separated by filtration, and the acetone was evaporated under dry nitrogen flow, weighed and stored at $-20^{\circ}C$ until subsequent fatty acids, triacylglycerol and DSC analyses. The yields (%w/w) of LF and SF were calculated for each T_C using Eqs. (1) and (2), respectively.

$$LF\ yield\ (\%) = \frac{Mass\ of\ LF\,(g)}{Mass\ of\ SBPO\ (g)} \times 100 \tag{1}$$

$$SF\ yield\ (\%) = \frac{Mass\ of\ SF\,(g)}{Mass\ of\ SBPO\,(g)} \times 100 \tag{2}$$

Analytical Methods

Fatty Acid Composition

Fatty acid compositions of the obtained LF and SF fractions were determined by GC. Samples were converted into their methyl esters (FAME) and analyzed on a 5890 series II gas chromatograph (Hewlett-Packard, Palo Alto, CA). The oven temperature was programmed as follows: isothermal for 1 min at 60°C, heating to 190°C at 20°C/min, and isothermal at this value for 30 min. The injector and detector temperatures were set at 250°C. Hydrogen was used as carrier gas. GC separation peaks was performed on a BPX-70 capillary column (60 m × 0.25 mm i.d. × 0.25 μm film thickness; SGE, Melbourne, Australia). Fatty acids were identified by comparing their retention times with those of FAME standards purchased from NuChek Prep (Elysian, MN, USA) under the same conditions. Peaks were integrated using Hewlett-Packard ChemStation software.

Triacylglycerol Composition

A gas chromatography (GC) method was used for the determination of the triacylglycerol (TAG) composition of the obtained LF and SF fractions as well as that of SBPO. Samples were dissolved in octane and analyzed on a 5890 gas chromatograph (Hewlett-Packard, Palo Alto, CA). The oven temperature was programmed as follows: from 250°C to 360°C at 3.0°C/min, and isothermal for 15 min at 360°C. Injector and detector temperatures were set at 400°C. Hydrogen was used as carrier gas. The GC separation method was performed on a RTX-65TG capillary column (30 m × 0.25 mm i.d. × 0.1 μm film thickness; Resteck, Bellefonte, PA, USA). The identification of the peaks was achieved by comparing their retention times with those of the standards purchased from Nu Chek Prep (Elysian, MN, USA) and Sigma-Aldrich (Sigma, St. Louis, MO, USA) under the same conditions. Peaks were integrated using Hewlett-Packard ChemStation software.

Melting and Crystallization Profiles

The melting profiles of the obtained LF and SF fractions as well as the crystallization curves of crude SBPO were determined by DSC using a differential scanning calorimeter (Pyris 1 DSC, Perkin Elmer, Norwalk, CT, USA) equipped with an intracooler II (Perkin Elmer, Norwalk, CT, USA). During analysis the system was purged with nitrogen at

30 mL/min. The melting curves were performed within the temperature range of -50°C to 50°C. Samples ($\sim$10 mg) were cooled to -50°C and held at this temperature for 5 min, then melted by heating at 5°C/min. The crystallization curves of the crude SBPO were carried out within the temperature interval of 50°C to -50°C. Samples were heated at 50°C and held at this temperature for 5 min, and then cooled at different cooling rates (0.1, 0.25, 0.5, 1.0, and 2.0°C/min). An empty pan was used as inert reference to balance the heat capacity of the sample pan. Calibration of DSC was carried out using indium ($mp = 156.6^{\circ}$C, $\Delta H_f = 28.71$ J/g). Data were analyzed using thermal analysis software (Pyris 1 Version 3.5, Perkin Elmer). The solid fat index (SFI) was determined from the DSC melting curves by sequential integration of peak areas (19,20).

Statistical Analysis

All assays were carried out in duplicate. Analysis of variance by the general linear models (GLM) procedure and mean comparisons by the least significant difference (LSD) test were performed using the Statistical Analysis System (21).

RESULTS AND DISCUSSION

Crystallization Profiles of the Crude SBPO

As depicted in Fig. 1, crystallization profiles of SBPO depend on the cooling rate. The crystallization curves performed at 1.0 and 2.0°C/min were characterized by the presence of one wide exothermic peak between -45°C and -3°C where its maximum is located at $\approx -4^{\circ}$C. In contrast, the crystallization profiles obtained at cooling rates of 0.25 and 0.5°C/min, showed a narrow exothermic peak between -7°C and 2°C, and -16°C and -2°C, respectively, which were formed by two well-defined overlapping peaks. Finally, when using a very low cooling rate (0.1°C/min), the crystallization curve exhibited a narrow sharp exothermic peak between -2°C and 4°C, thus highlighting finer fractional crystallization procedure at slower cooling of SBPO. Although the cooling rate of 0.1°C/min could result in very fine fractionation of triacylglycerols, carrying out the crystallization at 0.25°C/min was believed to be a good compromise between two opposing situations: fine fractionation

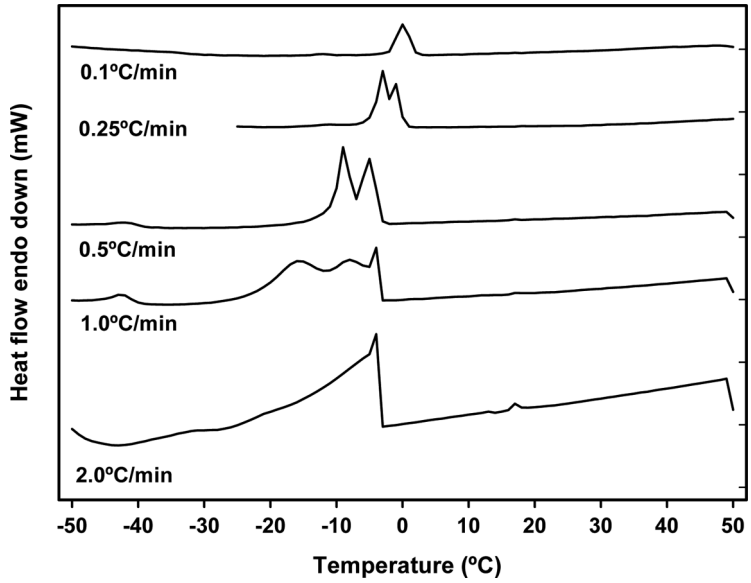

Figure 1. Crystallization curves of crude SBPO at different cooling rates.

obtained at very low cooling rate accompanied by long time processing and faster crystallization leading to the formation of impure crystals.

Fractions Yields

The effect of crystallization temperature (T_C) on the yields of LF and SF fractions obtained after solvent crystallization of crude SBPO is depicted in Fig. 2, in the range of -15 to 15°C. The choice of this range was based on the cooling curves of the mother liquor SBPO carried out at different cooling rates (0.1 to 2°C/min). The cooling curves showed that T_C could be located in the indicated interval. As shown, the crystallization temperature had a significant effect on the fractions yields. The increase of crystallization temperature enhanced the LF fraction yield, while it adversely affected the SF fraction yield. However, only slight differences were found between the yields of the LF and SF fractions obtained at $T_C = 15$°C (89.9 ± 0.2%w/w and 5.5 ± 0.8%w/w, respectively) and those attained at $T_C = 5$°C (92.8 ± 1.9%w/w and 5.5 ± 0.4%w/w, respectively). On the other hand, when T_C decreased from -5°C to -10°C, the yield of SF fraction doubled (62.0 ± 1.3%w/w vs. 31.3 ± 1, 0%w/w, $p < 0.05$), whereas that of LF fraction diminished by 50% (35.8 ± 0.3%w/w vs. 67.7 ± 0.9%w/w, $p < 0.05$).

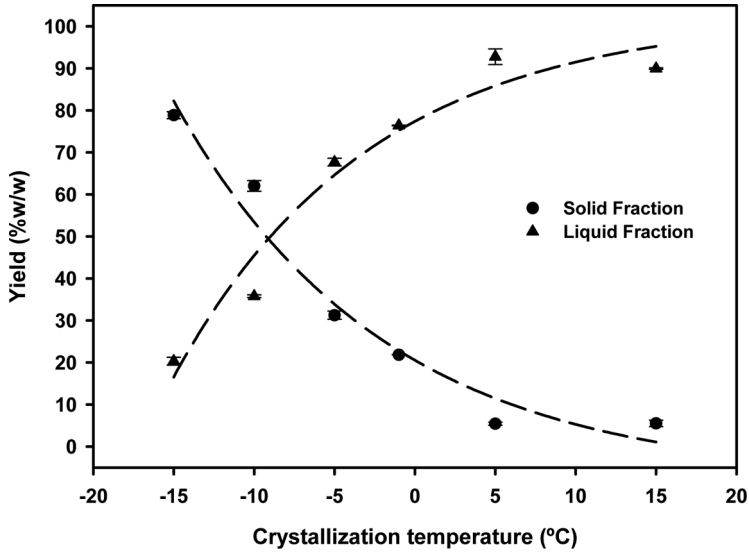

Figure 2. LF and SF fractions yields obtained after solvent crystallization of SBPO with acetone at different temperatures during 24 h, using a 1/5m/v oil to solvent ratio.

Fatty Acid Compositions of the Crude SBPO and its LF and SF

Table 1 presents the fatty acid profiles of the crude SBPO and its LF and SF fractions. As it can be seen, the crude oil was mainly rich in palmitoleic (C16:1, 41.4%), palmitic (C16:0, 34.7%) and linoleic (C18:2*n*-6, 10.2%) acids. Similar values were recently reported for seabuckthorn (cv. Indian-summer) pulp oil (12,22).

In LF fraction, it can be observed that except for palmitic, oleic, and arachidic acids, the concentrations of the other fatty acids increased as the crystallization temperature (T_C) decreased. Nevertheless, no significant differences were found between the fatty acid profiles of the crude SBPO, and those of the LF fraction obtained after fractionations carried out at 5°C and 15°C. When T_C decreased from 15 to −15°C, liquid fractions became poorer in saturated fatty acids (SFA, 37.9% to 19.1%), and richer in monounsaturated (MUFA, 51.0% to 65.5%) and polyunsaturated (PUFA, 11.1% to 13.8%) fatty acids. The crystallization carried out at T_C of −15°C diminished the proportion of palmitic acid by 60%, and increased the concentrations of palmitoleic and linoleic acids in LF fraction by circa 27 and 37%, respectively, if compared to the initial values of these fatty acids in crude SBPO. At this temperature,

Table 1. Fatty acid composition of the liquid and solid fractions obtained after solvent crystallization of sea buckthorn pulp oil with acetone at different temperatures during 24 h, using a 1/5m/v oil to solvent ratio[a]

	Fatty acids in liquid fractions									
T_C (°C)	C14:0	C16:0	C16:1	C17:0	C18:0	C18:1*n*-9	C18:1*n*-7	C18:2*n*-6	C18:3*n*-3	C20:0
−15	0.8^{a}	13.9^{a}	52.9^{a}	3.0^{a}	1.2^{a}	2.7^{a}	9.9^{a}	14.0^{a}	1.4^{a}	0.2^{a}
−10	0.6^{b}	22.2^{b}	48.3^{b}	2.5^{b}	1.0^{b}	3.0^{b}	8.5^{b}	12.5^{b}	1.3^{b}	0.2^{a}
−5	0.5^{c}	26.8^{c}	46.5^{c}	2.1^{c}	0.9^{b}	3.2^{c}	7.9^{c}	10.9^{c}	1.0^{c}	0.2^{a}
−1	0.5^{c}	28.8^{d}	45.1^{d}	2.1^{c}	1.0^{b}	3.1^{c}	7.5^{d}	10.7^{c}	1.0^{c}	0.2^{a}
5	0.4^{d}	34.6^{e}	41.4^{e}	2.0^{d}	0.9^{c}	3.1^{c}	6.5^{e}	10.1^{d}	1.0^{c}	0.2^{a}
15	0.4^{d}	34.6^{e}	41.4^{e}	1.9^{de}	0.8^{c}	3.1^{c}	6.5^{e}	10.1^{d}	1.0^{c}	0.2^{a}
	Fatty acids in solid fractions									
−15	0.3^{a}	39.6^{a}	39.1^{a}	1.7^{a}	0.8^{a}	3.1^{ab}	5.6^{a}	9.0^{a}	0.8^{a}	0.2^{a}
−10	0.3^{a}	40.3^{a}	38.1^{b}	1.7^{a}	0.8^{a}	3.1^{a}	5.6^{a}	9.1^{a}	0.9^{b}	0.2^{a}
−5	0.2^{b}	53.0^{b}	29.3^{c}	1.5^{b}	0.3^{b}	2.8^{c}	3.3^{b}	8.3^{b}	0.9^{b}	0.1^{b}
−1	0.1^{c}	58.1^{c}	26.4^{d}	1.4^{c}	0.4^{c}	2.9^{cd}	2.4^{c}	7.5^{c}	0.8^{a}	0.1^{b}
5	0.4^{d}	33.9^{de}	40.4^{e}	2.0^{d}	0.8^{a}	3.0^{e}	6.6^{d}	11.0^{d}	1.6^{c}	0.2^{a}
15	0.3^{d}	33.0^{d}	39.1^{a}	2.1^{e}	0.8^{a}	2.9^{d}	7.0^{e}	13.0^{e}	1.4^{d}	0.3^{c}
	Fatty acids in crude oil									
	0.4	34.7	41.4	1.9	0.9	3.0	6.5	10.2	0.9	0.2

[a]For each fraction, means in a column followed by the same letter are not significantly different by LSD test at the 5% level.

the concentration of palmitoleic acid in LF fraction was slightly higher (52.9% vs. 52.1%) while that of palmitic acid was significantly lower (13.9% vs. 40%), in comparison to the results reported by Rüsch gen. Klaas and Meurer for the same product (10). On the other hand, when the temperature decreased from 5 to $-15^{\circ}C$, the proportion of palmitic acid showed a negative correlation with that of palmitoleic ($R^2 = 0.99$, $p < 0.0001$), linoleic ($R^2 = 0.96$, $p < 0.001$), and vaccenic ($R^2 = 0.99$, $p < 0.0001$) acids.

In SF fraction, it can be noticed that except for palmitic acid, the concentration of the other major fatty acids decreased until their lower values at $T_C = -1^{\circ}C$, then they increased as T_C decreased further. The concentration of the minor ones remained quasi-unchanged. The crystallization process at $-1^{\circ}C$ yielded 21.9%w/w of a solid fraction with the highest concentration of SFA (60.1%), and lowest proportions of MUFA and PUFA (31.6% and 8.3%, respectively). At this temperature, concentration of palmitic acid increased by *circa* 67%, while the proportions of palmitoleic and linoleic acids diminished by 36% and 26% respectively, in comparison to their initial values in crude SBPO. Palmitic acid reached its higher concentration (58.1%) at $T_C = -1^{\circ}C$, whereas palmitoleic and linoleic acids attained 26.4% and 7.5%, respectively.

Triacylglycerol Composition of the Crude SBPO and its LF and SF

The TAG compositions of the crude SBPO and its LF and SF fractions obtained at different T_C are presented in Table 2. The crude oil contained mainly TAGs with acyl carbon number (ACN) of 48 and 50, both representing approximately 95% of the total TAGs (57.1% and 38.2%, respectively). TAGs of 48 acyl carbons with 2 double bonds (DB) (i.e. 48:2) constituted the major ACN:DB of these TAG species, followed by 48:1 and 48:3 (29.0%, 19.6%, and 8.4%, respectively). In the case of TAGs having 50 acyl carbons, the most abundant ACN:DB were 50:2 and 50:3 (15.5% and 13.8%, respectively). The patterns of the molecular weight distribution of TAG of the crude SBPO obtained in this study were in accordance with those reported recently by Yang and Kallio (23) for berries of sea buckthorn of different origins. According to these authors, TAG species of ACN:DB 48:1 and 48:2 are constituted mainly by a combination of palmitoleic and palmitic acids, whereas TAG species of ACN:DB 50:2 and 50:3 corresponded mostly to two major fatty acids combinations: 16:1/16:0/18:1 and 16:0/16:0/18:2, for TAGs 50:2; and 16:1/16:1/18:1 and 16:1/16:0/18:2 for TAGs 50:3.

As it can be seen in Table 2 for LF fraction, the overall TAG species with 48 acyl carbons decreased (57.1% to 38.2%) while those with 50 acyl

Table 2. Triacylglycerol composition of the liquid and solid fractions obtained after solvent crystallization of sea buckthorn pulp oil with acetone at different temperatures during 24 h, using a 1/5m/v oil to solvent ratio[a]

	TAG in liquid Fractions													
T_C (°C)	C46:1	C46:2	C48:1	C48:2	C48:3	C50:0	C50:1	C50:2	C50:3	C50:4	C50:5	C52:2	C52:3	C52:4
−15	0.1^{d}	1.0^{d}	0.9^{f}	15.0^{e}	22.3^{d}	2.2^{d}	0.4^{f}	6.5^{d}	24.5^{f}	13.0^{e}	1.8^{b}	0.5^{a}	4.8^{c}	6.9^{d}
−10	0.2^{cd}	0.7^{c}	3.2^{e}	26.7^{b}	14.4^{d}	1.3^{c}	1.3^{e}	11.9^{c}	21.2^{e}	7.9^{d}	1.0^{a}	1.4^{bc}	4.6^{c}	4.2^{c}
−5	0.4^{ab}	0.5^{b}	4.8^{d}	33.0^{d}	10.5^{c}	1.0^{a}	1.7^{e}	14.8^{b}	18.7^{d}	5.7^{c}	0.7^{a}	1.7^{cd}	4.0^{bc}	2.6^{b}
−1	0.4^{ab}	0.5^{b}	8.1^{c}	30.7^{c}	9.6^{b}	0.9^{ab}	2.4^{b}	15.4^{b}	17.4^{c}	5.6^{c}	0.7^{a}	1.9^{d}	3.7^{bc}	2.7^{b}
5	0.3^{bc}	0.3^{a}	17.9^{b}	26.8^{b}	8.2^{a}	1.0^{a}	3.7^{a}	15.8^{a}	14.9^{b}	4.4^{b}	0.6^{a}	1.3^{bc}	2.8^{ab}	1.8^{ab}
15	0.4^{ab}	0.4^{ad}	17.7^{b}	26.6^{b}	8.2^{a}	0.8^{a}	3.8^{a}	15.9^{a}	14.7^{b}	4.4^{b}	0.7^{a}	1.8^{cd}	2.9^{ab}	1.9^{ab}
	TAG in solid fractions													
−15	0.4^{bc}	0.2^{acd}	21.6^{f}	29.8^{ab}	5.3^{d}	0.5^{b}	4.4^{b}	17.5^{e}	12.5^{be}	2.3^{e}	0.4^{c}	1.4^{a}	2.3^{c}	1.4^{bd}
−10	0.4^{bc}	0.3^{ac}	24.5^{e}	26.9^{c}	5.6^{d}	0.5^{b}	4.9^{b}	17.4^{de}	11.9^{e}	2.5^{e}	0.4^{c}	1.2^{a}	2.2^{ac}	1.2^{b}
−5	0.3^{c}	0.1^{d}	47.8^{d}	13.1^{e}	3.3^{c}	0.3^{b}	8.4^{d}	17.1^{d}	5.9^{d}	1.3^{d}	0.2^{b}	0.5^{bc}	0.8^{bd}	0.5^{ce}
−1	0.3^{c}	0.2^{cd}	54.3^{c}	9.5^{d}	2.3^{b}	0.4^{b}	10.2^{c}	16.7^{c}	3.9^{c}	0.6^{c}	0.2^{b}	0.3^{c}	0.4^{d}	0.3^{e}
5	0.3^{bc}	0.3^{ac}	18.3^{b}	27.0^{c}	8.3^{a}	0.8^{a}	3.7^{a}	15.7^{a}	14.7^{a}	4.0^{a}	0.7^{a}	1.6^{a}	2.5^{c}	1.8^{d}
15	0.6^{a}	0.7^{b}	20.1^{a}	30.1^{b}	8.5^{a}	0.9^{a}	4.6^{b}	15.0^{b}	12.8^{b}	3.1^{b}	0.6^{a}	1.0^{ab}	1.1^{b}	0.7^{ac}
	TAG in crude oil													
	0.5	0.4	19.6	29.0	8.4	0.8	3.7	15.5	13.8	3.7	0.7	1.0	1.9	1.1

[a]For each fraction, means in a column followed by the same letter are not significantly different by LSD test at the 5% level.

carbons increased (38.2% to 48.4%) when T_C decreased from 15°C to −15°C. However within TAG species with 48 acyl carbons, ACN:DB 48:1 and 48:2 diminished, whereas ACN:DB 48:3 increased. A similar behavior was shown by the TAG species with 50 acyl carbons. ACN:DB 50:1 and 50:2 diminished, contrary to ACN:DB 50:3, 50:4, and 50:5, which increased. Thus, within the range of investigated temperatures (15° to −15°C), the decrease in palmitic acid concentration of LF fraction correlates pretty well ($R^2 = 0.97$, $p = 0.0003$) with the decrease of the overall amount of the TAG species ACN:DB 48:1, 48:2, 50:1, and 50:2. This may be attributed to the possible presence of this fatty acid in these TAG species. On the other hand, the crystallization process at −15°C diminished the monounsaturated TAG species from 23.8% to 1.4%, and amplified the proportion of polyunsaturated TAG species from 75.4% to 96.3%, when comparing the obtained results to those of same TAG species present in crude SBPO.

The concentrations of TAG species in SF fraction are shown in Table 2. It can be observed at $T_C = -1$°C, that TAG species with 48 acyl carbons accounted for 66.1%, while those of 50 acyl carbons represented only 31.9%. Within these TAG species, the ACN:DB 48:2, 48:3, 50:3, 50:4, and 50:5 diminished as T_C decreased to −1°C, whereas ACN:DB 48:1, 50:1, and 50:2 increased. Thus, after the crystallization at $T_C = -1$°C, a solid fraction with the highest concentration of monounsaturated TAG species and the lowest proportions of polyunsaturated TAG species (64.8% and 34.5%, respectively) can be recovered.

Melting Profiles of the Crude SBPO and its LF and SF Fractions

Figures 3a and 3b show the melting profile curves recorded using DSC, when heating the crude SBPO and its liquid and solid fractions at 5°C/min from −50 to 50°C. Melting of crude SBPO started at approximately −26°C with a broad endotherm which spanned until −7°C. This low-temperature endotherm (LTE), whose peak maximal temperature (T_m) and melting enthalpy (H_m) were about −23.5°C and 24 J/g respectively, corresponds to the low-melting triacylglycerols (LMT) of the SBPO. A middle-temperature endotherm (MTE), mainly corresponds to the melting of medium chain triacylglycerols (MMT), extends from −7°C to circa 7°C, with a T_m of −3.7°C, and H_m of 16 J/g. The main peak of the MTE was followed by two minor transitions at ≈0°C and 4°C, prior to the melt beginning of the high-melting triacylglycerols (HMT) chains. These TAGs exhibited a prominent endothermic peak between 7°C and 17°C, with a T_m of approximately 11°C, and H_f of

30 J/g. The average total melting enthalpy (ΔH) of the crude SBPO was evaluated to 75 J/g. According to Timms (24), the large area of the high-temperature endotherm (HTE) would be partly due to the higher melting heat of the HMT and their co-crystallization with the lower melting triacylglycerols in a semi-stable mixture.

As shown in Figs. 3a and 3b, the solvent crystallization process induced marked changes in the thermal characteristics of the liquid and solid fractions obtained after the crystallization process at -1°C, -5°C, and -15°C, compared to the crude SBPO. The melting curve of the LF obtained at $T_C = -1$°C (Fig. 3a) presents a broad endothermic peak between -23°C and -3°C ($T_m = -18$°C), followed by a second prominent endothermic peak spanned between -3°C and 13°C ($T_m = 9$°C). For this fraction, the average total melting enthalpy (ΔH) was nearly 74 J/g. On the other hand, the melting behavior of the LF obtained at $T_C = -5$°C showed two well defined and separated endothermic peaks. The first, between -23°C and -10°C had a $T_m = -17.6$°C, whereas the second, between circa -8°C and 10°C had a $T_m = 6.9$°C. The ΔH for this fraction was approximately 67 J/g. When melting, the LF fraction obtained at $T_C = -15$°C exhibited two overlapping peaks between -30°C and -18°C ($T_m = -22.5$°C), and between -18°C and -10°C ($T_m = -13.1$°C), with an average total melting enthalpy (ΔH) of about 62 J/g. Thus, as shown in Fig. 3a, the liquid fractions obtained after solvent crystallization processes at -1°C and -5°C were mainly impoverished in HMT, contrary to the liquid fraction obtained at $T_C = -15$°C, which was mainly enriched in LMT.

Figure 3b presents the melting profiles of the solid fractions obtained after crystallization carried out at -1°C, -5°C and -15°C. The melting curves of the SF obtained at -1°C and -5°C were characterized by the presence of one broad exothermic peak between -19°C and 3°C ($T_m = -3.5$°C) and between -20°C and 0°C ($T_m = -12.8$°C) respectively, before the melting of their HMT highlighted by the prominent endothermic peaks between 15°C and 27°C ($T_m = 25.7$°C), and between 6°C and 25°C ($T_m = 22$°C), respectively. The average total melting enthalpies (ΔH) of the SF obtained after crystallization processes at -1°C, -5°C and -15°C were 78.1, 75.1, and 75.7 J/g, respectively.

Fractionation Efficiency of SBPO Using Solvent Crystallization

The difference in the melting points (MP) between LF and SF fractions, as represented by Eq. (3), can be regarded as an indicator of SBPO fractionation efficacy. The higher this difference, the better is the fractionation, and the greater is the effectiveness of separation between the two

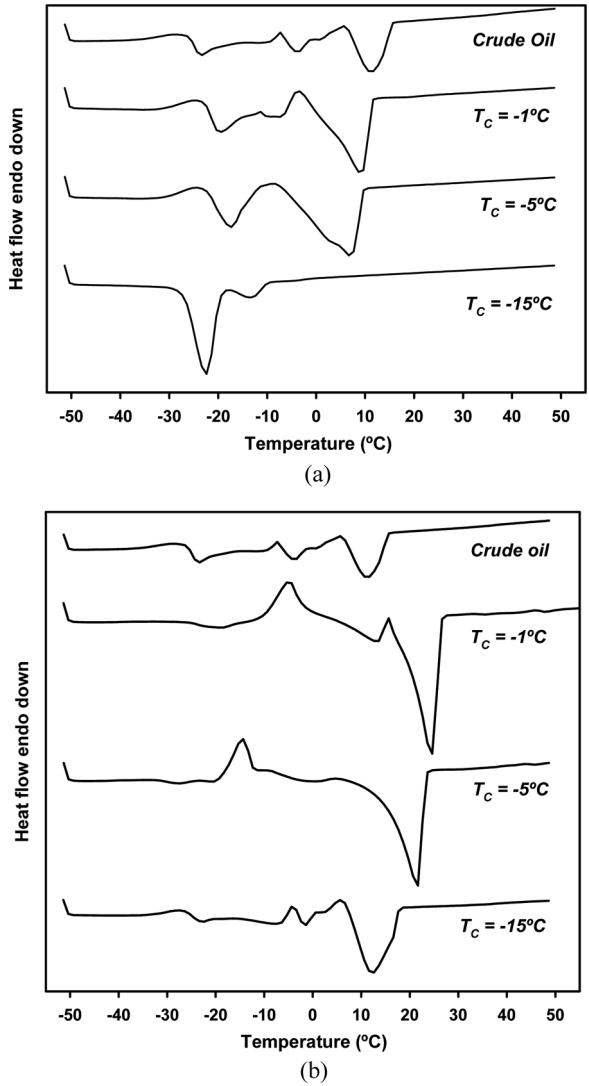

Figure 3. Melting curves of crude SBPO and their LF (a) and SF (b) fractions obtained after solvent crystallization with acetone at different temperatures during 24 h, using a 1/5m/v oil to solvent ratio (Heating rate = 5°C/min).

fractions. This criterion was previously introduced to describe successfully the fractionation efficacy of anhydrous milk fat by dry crystallization process (25).

$$\Delta MP = MP_{SF} - MP_{LF} \quad (3)$$

In the present work, the melting points of the obtained fractions *via* fractional solvent crystallization of SBPO were approximated by taking the temperature corresponding to the end of last endothermic pick of the fractions melting curves acquired by DSC.

In the SBPO fractionation by the solvent crystallization process, the crystallization temperature appears to have a significant effect on the separation efficacy. Strong difference approaching 26°C in melting points of LF and SF fractions was obtained at $T_C = -15$°C indicating an excellent separation between these fractions (See Fig. 4). Near and beyond $T_C = -10$°C, the SBPO fractionation is less effective and remains insensitive to the crystallization temperature changes. It is thought that this loss of fractionation efficacy is ascribed to the inadequate supercooling gradient favouring the occlusion of mother liquor oil or low-melting TAGs into the crystal matrix.

Solid Fat Index of the Crude SBPO and its LF and SF

Figure 5a shows the solid fat index (SFI) of the crude SBPO and its liquid fractions obtained after crystallization processes at −1°C, −5°C, −10°C,

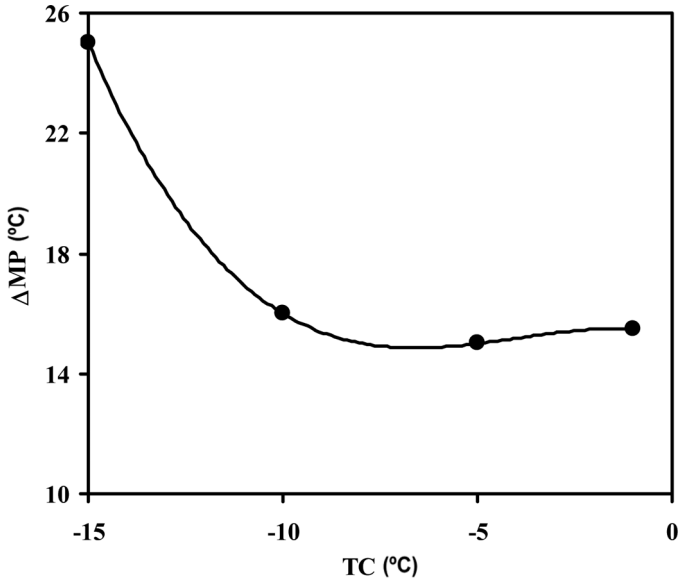

Figure 4. Effect of the crystallization temperature on the SBPO fractionation efficiency.

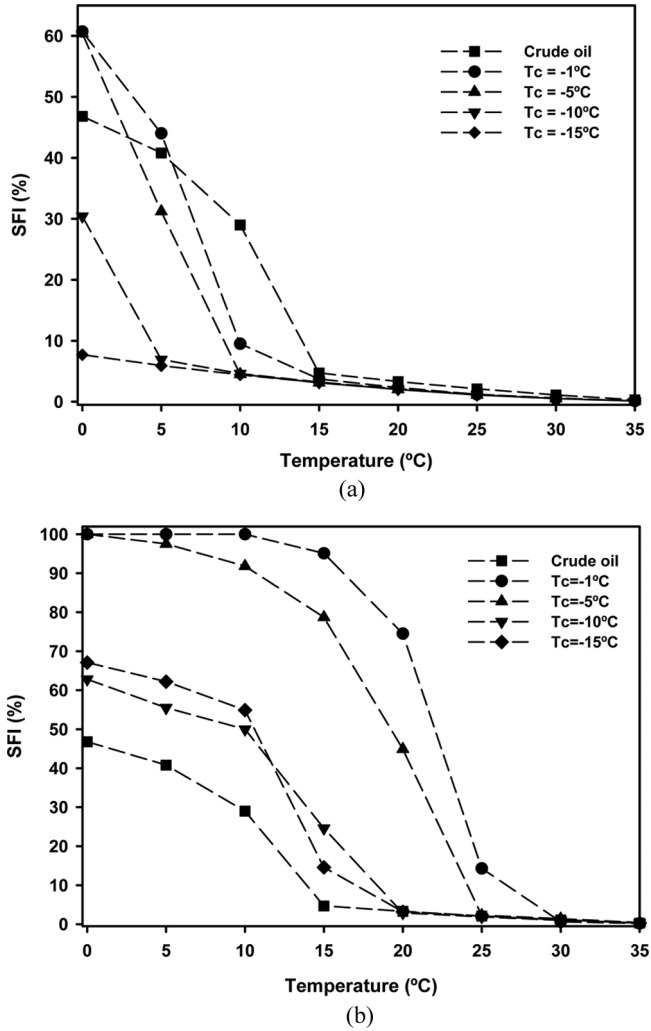

Figure 5. Solid fat index (g/100 g) of the crude SBPO and their LF (a) and SF (b) fractions obtained after solvent crystallization processes with acetone at different temperatures (Values obtained from the DSC melting curves using a heating rate of 5°C/min).

and −15°C, as a function of melting temperature. As it can be observed, the SFI values of the crude SBPO and its liquid fractions decrease as the melting temperature increases. Crude SBPO have a SFI at 0°C of about 47%, and it melted sharply between 5–15°C. The LF obtained at −1°C

and −5°C exhibited SFI values significantly greater than those exhibited by the crude SBPO at 0°C, but over this temperature, these fractions showed a curt drop in their SFI, and melted almost completely at temperatures above 15°C. On the other hand, the unsaturated nature of the LF fractions obtained at −10°C and −15°C is highlighted when observing their SFI profiles. These fractions had very low SFI values at 0°C. Similarly to the crude SBPO and the other liquid fractions, they melted completely above 15°C.

Figure 5b presents the SFI of the crude SBPO and its solid fractions obtained after crystallization processes at −1°C, −5°C, −10°C, and −15°C as a function of melting temperature. As illustrated, at temperatures under 20°C, the SFI values of the crude SBPO were much lower than those obtained for its solid fractions. On the other hand, because of the exothermic transition exhibited in their melting profiles (see Fig. 5b), the SF fractions obtained at −1°C and −5°C showed the highest SFI values, when compared to those of crude SBPO and the SF fractions obtained at −10°C and 15°C. The semisolid nature of these fractions at −20°C could make them valuables ingredients for shortening formulations. On the other hand, the SF obtained at −10°C and −15°C presented similar SFI profiles. At 10°C these fractions have about 50% of solid fat, and above this temperature they melted rapidly to become almost completely liquid at temperatures over 20°C.

CONCLUSIONS

The enrichment of SBPO in health-beneficial palmitoleic acid and simultaneous minimizing its content in non-desirable palmitic acid, preserving the chemical nature of the oil in triacylglycerol (TAG) form was revealed possible by solvent fractionation process. Good quality crystallization yielding two distinct and well-separated lipid fractions was accomplished when using a cooling rate of 0.25°C/min at reasonable processing time. The crystallization temperature had a major effect not only on the fractions yields but also on the fractionation efficacy and products quality. Fractionation at −15°C yielded about 20%w/w of LF with the highest and lowest concentrations of UFA and SFA (80.9% and 19.1%, respectively). At this temperature, palmitoleic and palmitic acids were 52.9% and 13.9%, respectively. On the contrary, the solid fraction was characterized by the presence of high-melting lipids of saturated nature with high concentrations of mainly palmitic acid. All the TAG molecules found in the crude SBPO were present in both liquid and solid fractions, but their proportions were different, as a result of unambiguous fractionation obtained by solvent crystallization process. LF fractions were richer

in TAG molecules with acyl carbon number of 48 having 2 and 3 double bounds (C48:2 and C48:3) than SF ones, which contained higher amounts of C48:1, C50:2, and C50:2. The crystallization process caused marked changes in the thermal characteristics and melting behavior of the initial SBPO. The melting curves demonstrated the more unsaturated nature for the LF fraction and saturated nature of the SF fraction and confirmed the TAG separation of low melting point formed by unsaturated fatty acids from those of higher melting point formed essentially by saturated fatty acids.

To the best of our knowledge, it is the first time that the enrichment in palmitoleic acid of sea buckthorn pulp oil was attempted successfully without destroying the intrinsic chemical character of the triacylglycerols (TAG) present in this oil.

ACKNOWLEDGMENTS

This research was funded by the Natural Sciences and Engineering Research Council of Canada (NSERC), the "Association des Producteurs d'Argousier du Québec" (APAQ), and the Nutraceuticals and Functional Foods Institute (INAF) of the Université Laval. We express our sincere thanks to André Nicole for providing the seabuckthorn berries.

REFERENCES

1. Yamori, Y., Nara, Y., Tsubouchi, T., Sogawa, Y., Ikeda, K., Horie, R. (1986) Dietary prevention of stroke and its mechanisms in stroke-prone spontaneously hypertensive rats. Preventive effect of dietary fiber and palmitoleic acid. *J. Hypertens.*, *4*: S449.
2. Cummings, M. (1999) Macadamia nut oil. *Cosmet. Toiletries.*, *114*: 75.
3. Gutiérrez, L-F. (2006) Extraction et caractéristiques des huiles de l'argousier (*Hippophaë rhamnoides* L.). Une étude des effets de la méthode de déshydratation des fruits sur le rendement d'extraction et la qualité des huiles MSc Thesis, U Laval.
4. Yang, B.; Gunstone, F.D.; Kallio, H. (2003) Palmitoleic Acid. In: *Lipids for Functional Foods and Nutraceuticals*, Gunstone, F.D., ed.; Oily Press: Bridgwater, U.K.
5. Wille, J.J., Kydonieus, A. (2003) Palmitoleic acid isomer (C16: 1 Delta 6) in human skin sebum is effective against gram-positive bacteria. *Skin Pharmacol. Appl. Skin Phys.*, *16*: 176.
6. Welters, H.J., Diakogiannaki, E., Mordue, J.M., Tadayyon, M., Smith, S.A., Morgan, N.G. (2006) Differential protective effects of palmitoleic acid and

cAMP on caspase activation and cell viability in pancreatic beta-cells exposed to palmitate. *Apoptosis*, *11*: 1231.
7. Kolonel, L N. (2001) Fat, meat, and prostate cancer. *Epidemiol. Rev.*, *23*: 72.
8. Kolonel, L.N., Nomura A.M.Y., Cooney Robert, V. (1999) Dietary fat and prostate cancer: Current status. *J. National Cancer Inst.*, *91*: 414.
9. Pandian, S.S., Eremin, O.E., McClinton, S., Wahle, K.W.J., Heys, S.D. (1999) Fatty acids and prostate cancer: Current status and future challenges. *J. R. Coll. Surg. Edinb.*, *44*: 352.
10. Heilscher, K., Lorber, S. (1996) Cold working process for obtaining clear juice, sediment and oil from seabuckthorn berries and their use. German Patent DE 4431394 C1.
11. Rüsch gen. Klaas, M., Meurer, P.U. (2004) A palmitoleic acid ester concentrate from sea buckthorn pomace. *Eur. J. Lipid Sci. Tech.*, *106* (7): 412.
12. Canas, B.J., Yurawecz, M.P. (1999) Ethyl carbamate formation during urea complexation for fractionation of fatty acids. *J. Am. Oil Chem. Soc.*, *76* (4): 537.
13. Gutiérrez, L.-F., Ratti, C., Belkacemi, K. (2008) Effects of drying method on the extraction yields and quality of oils from Quebec sea buckthorn (*Hippophaë rhamnoides* L.) seeds and pulp. *Food Chem.*, *106* (3): 896.
14. O'Shea, M., Devery, R., Lawless, F., Keogh, K., Stanton, C. (2000) Enrichment of the conjugated linoleic acid content of bovine milk fat by dry fractionation. *Int. Dairy J.*, *10* (4): 289.
15. Timms, R.E. (2005) Fractional crystallization – the fat modification process for the 21st century. *Eur. J. Lipid Sci. Tech.*, *107* (1): 48.
16. Mohamed, H.M.A. (1999) Characterization of the high-melting glyceride fraction isolated from cottonseed oil stearin by fractional crystallization in isopropanol. *Fett-Lipid*, *101* (1): 20.
17. Yokochi, T., Usita, M.T., Kiamisaka, Y., Nakahara, T., Suzuki, O. (1990) Increase in the γ-linolenic acid content by solvent winterization of fungal oil extracted from mortierella genus. *J. Am. Oil Chem. Soc.*, *67* (11): 846.
18. Vanputte, K.P., Bakker, B.H. (1987) Crystallization kinetics of palm oil. *J. Am. Oil Chem. Soc.*, *64* (8): 1138.
19. Deroanne, C. (1977) L'analyse calorimétrique différentielle, son intérêt pratique pour le fractionnement de l'huile de palme et la détermination de la teneur en phase solide. *Lebensmittel-Wissenschaft & Technologie.*, *10* (5): 251.
20. Lambelet, P. (1983) Comparison of NMR and DSC methods for determining solid content of fats application to milk-fat and its fractions. *Lebensmittel-Wissenschaft & Technologie.*, *16* (2): 90.
21. SAS Institute. (2000) *SAS/STAT User's Guide, Version 8*. SAS Institute Inc., Cary, NC.
22. Cenkowski, S., Yakimishen, R., Przybylski, R., Muir, W.E. (2006) Quality of extracted seabuckthorn seed and pulp oil. *Canadian Biosystems Engineering.*, *48*: 39.
23. Yang, B.R., Kallio, H. (2006) Analysis of triacylglycerols of seeds and berries of sea buckthorn (*Hippophae rhamnoides*) of different origins by mass spectrometry and tandem mass spectrometry. *Lipids*, *41* (4): 381.

24. Timms, R.E. (1980) The phase behavior and polymorphism of milk-fat, milk-fat fractions and fully hardened milk-fat. *Aust. J. Dairy Technol.*, *35* (2): 47.
25. Belkacemi, K., Angers, P., Fisher, O., Arul, J. (2003) Fractionation of milk fat by falling film layer crystallization. *Sep. Sci. Technol.*, *38* (12&13): 3115.